Vol. 52: 233–244, 2008
doi: 10.3354/ame01231

AQUATIC MICROBIAL ECOLOGY
Aquat Microb Ecol

Printed September 2008
Published online September 3, 2008

Constraints on viral production in the Sargasso Sea and North Atlantic

Janet M. Rowe[1], Matthew A. Saxton[1], Matthew T. Cottrell[2], Jennifer M. DeBruyn[3], G. Mine Berg[4], David L. Kirchman[2], David A. Hutchins[2,5], Steven W. Wilhelm[1,*]

[1]Department of Microbiology, University of Tennessee, Knoxville, Tennessee 37922, USA
[2]College of Marine and Earth Studies, University of Delaware, Lewes, Delaware 19958, USA
[3]Department of Ecology and Evolutionary Biology, University of Tennessee, Knoxville, Tennessee 37922, USA
[4]Department of Geophysics, Stanford University, Stanford, California 94305, USA
[5]Department of Biological Sciences, University of Southern California, Los Angeles, California 90089, USA

ABSTRACT: During the spring of 2005, the production rate of virus-like particles as well as microbial and biogeochemical parameters in the Sargasso Sea and North Atlantic Ocean were investigated as part of a multifaceted North Atlantic Spring Bloom (NASB2005) survey. Here we present data on the spatial variations in viral production rate, abundance, and infection of microbial host populations, in an attempt to understand the constraint(s) on the rates of viral production and abundance. As expected, virus-like particle densities increased from the oligotrophic waters of the Sargasso Sea to the more productive northern Atlantic waters. Additionally, viral production rates increased across the Sargasso Sea transect and correlated with trophic status (chl *a* concentrations) and secondary (bacterial) productivity in this region. However, no clear pattern of viral production rates could be discerned in waters hosting the NASB. Results of both parametric and non-parametric analyses demonstrate that viral production rates and abundances only correlate well for our observations within the constant 'stability' of the Sargasso Sea, but suggest that more complex relationships including a threshold effect, may guide viral parameters in the North Atlantic. Overall, this study highlights the spatial and potentially temporal complexity of constraints on viral production and ultimately on viral function in surface marine waters.

KEY WORDS: Spring bloom · Marine · Virus · Microbes · Nutrients

INTRODUCTION

Although viruses have been recognized as agents of bacterial mortality for nearly a century (Duckworth 1976), their role in the environment has come under study only recently. Present evidence suggests that viruses play a critical role in the microbial loop of both freshwater (DeBruyn et al. 2004) and marine systems (Wilhelm & Suttle 1999, Suttle 2005). As obligate pathogens, viruses release previously fixed carbon in forms which are bioavailable to co-existing heterotrophs (Fuhrman 1992). Moreover, nutrients like N, P, Se and Fe (Gobler et al. 1997, Poorvin et al. 2004, Mioni et al. 2005), and even amino acids (Middelboe & Jörgensen 2006) can be made bioavailable to microbial community members after viral lysis of host cells. Aquatic viruses are also thought to influence the structure of microbial populations through the 'kill the winner' mechanism, i.e. by controlling abundances of dominant community members, allowing less competitive members to survive (Thingstad & Lignell 1997). As such, it is apparent that viruses may influence community diversity during the establishment, proliferation and decline phases of any microbial population (Brussaard et al. 2008).

Much of our current knowledge concerning virus–host interactions and distributions in marine environments is derived from studies conducted on local spatial scales (~10s of km). Few studies have focused on temporal changes and fewer still have examined

*Corresponding author. Email: wilhelm@utk.edu

viral parameters on oceanic scales (1000s of km). To answer questions concerning the global impact of viruses on marine ecosystems and identify constraints on viral activity, we must first examine virus-associated parameters over these larger spatial regions. Viral abundances and viral decay rates have previously been examined over a ~5000 km transect along the western coast of South America (Wilhelm et al. 2003). That study distinguished the effects of both latitudinal gradients in light and localized ocean physics (e.g. upwelling) on communities. However, factors such as viral production rate and burst size (the abundance of viruses released per lytic event) have yet to be measured over such large distances.

No detailed process study on the NASB has been conducted since the end of the JGOFS North Atlantic Bloom Experiment in 1989/1990, despite the generally recognized biogeochemical importance of this occurrence. Early studies focused primarily on phytoplankton and parameters of photosynthesis (Sieracki et al. 1993, Balch et al. 1996). Typically, early blooms of diatoms are succeeded by coccolithophorids towards the later stages of the bloom, likely due to factors such as the changing availability of nutrients. These changes in the structure of the pelagic food chain can alter the diversity of higher trophic levels.

During a 2005 cruise to the spring bloom, we estimated parameters associated with viral infection and production rates as we transited from the oligotrophic Sargasso Sea to the more eutrophic North Atlantic. A study bridging these 2 contrasting regimes provides a unique opportunity to see how biotic and abiotic parameters influence viral distributions, production rates, and estimates of lytic burst sizes. The results provide insights into processes across large spatial scales, and through natural transitions between 2 regimes of contrasting stability and trophic status.

MATERIALS AND METHODS

Cruise logistics. Samples were collected while on board the RV 'Seward Johnson' at 15 underway stations in the Sargasso Sea, and at 54 'process' stations in the North Atlantic. On the Sargasso transit leg between Florida and the Azores (a non-stop 'deadhead' transit), daily samples were taken underway from the ship's clean surface pump (~5 m) as well as from a single depth profile. On the North Atlantic transect from the Azores to Iceland, station locations were chosen based on satellite images indicating coccolithophorid blooms. On this leg, daily water column profiles were taken in the morning from 2 CTD casts; one shallow (with samples collected from 5 to 50 m) and one deep (with samples collected from 70 to 200 m). Salinity, water temperature, *in situ* fluorescence (a proxy for chl *a*), pressure, density, conductivity, oxygen, oxygen saturation, and SPAR (surface PAR) were all measured using the CTD package mounted on the rosette sampler. Data presented herein are from surface (5 m) water samples, and have been limited to those that correspond with 32 viral production assays that were carried out (discussed below). Fig. 1 shows the locations where assays were done.

Chlorophyll *a*. Size-fractionated chl *a* concentrations were determined on replicate samples collected on 0.22, 2.0, and 20.0 µm nominal pore size, 47 mm diameter polycarbonate filters (Osmonics). Samples were extracted in 90% acetone for 24 h at 4°C and quantified using a solid-standard normalized 10-AU field fluorometer (Turner Designs) using the non-acidification protocol (Welschmeyer 1994).

Viral abundance. The abundance of viral particles was determined for whole water samples which were preserved in 2% final glutaraldehyde and then processed immediately at sea (Wen et al. 2004). Slide preparation involved staining 850 µl of sample with SYBR Green (Noble & Fuhrman 1998). All slides were stored at –20°C until virus-like particles could be enumerated via epifluorescence microscopy using a Leica DMRXA with a 'wide blue' filter set (λ_{Ex} = 450 to 490 nm, λ_{Em} = 510 nm, with suppression filter at λ = 510 nm). For each slide, >20 independent fields were

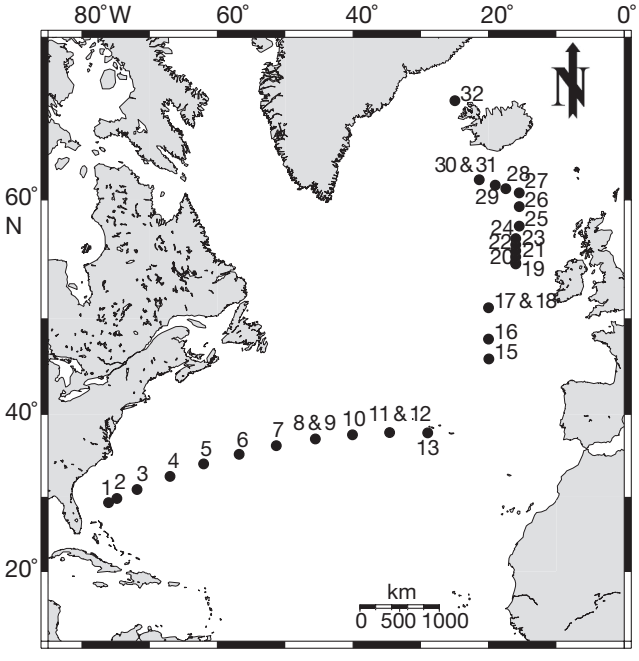

Fig. 1. Locations where viral production estimates and corresponding measurements were completed. Numbers 1 to 13 correspond to stations within the Sargasso Sea; Numbers 15 to 32 correspond to stations within the North Atlantic

viewed with the total of each grid noted to ensure particles were evenly distributed across individual filters. Standard deviations were calculated from the range of counts per field per slide.

Viral production. Viral production was estimated based on the virus reduction assay (Wilhelm et al. 2002) with abundances for each time point enumerated as described above. Four of the dilutions were prepared using a Millipore lab scale tangential flow filtration system with 0.22 µm filter cartridges (vis-a-vis Winget et al. 2005), although we have subsequently seen no difference between these 2 approaches (dead-end vs. tangential flow filtration, not shown). Briefly, 500 ml of sample water was reduced over a 0.22 µm filter (either dead-end or tangential flow filtration), reducing free viral particles and briefly concentrating the cellular community. Cells were resuspended in 500 ml of ultrafiltrate (free of viral particles) and divided into three 150 ml samples within 250 ml clear bottles. Samples for viral particle and cell enumeration were taken every 2.5 h for a period of 10 h. Bottles were incubated in on-deck flow seawater incubators under ambient daylight attenuated through blue-tinted acrylic to simulate natural temperatures and light penetration through surface waters. Ultrafiltrate was generated from surface water from the same station where each viral production sample was taken. Standard deviations of production rate were calculated from the averaged slopes of independent triplicate samples (data plotted as virus-like particles over time).

Burst size and percentage of infected cells. A 50 ml sample of the whole water used for viral production estimation was preserved immediately with 2% glutaraldehyde (final) and stored at 4°C until processing (~2 mo post-cruise). Approximately 30 ml of sample was centrifuged onto carbon-coated collodian films on top of 400 mesh copper grids and each sample-laden grid then stained with 0.75% uranyl formate. Grids were examined using 100KeV on a Hitachi H-800 transmission electron microscope under magnifications of 15 000 to 20 000× to scan over samples, 30 000 to 40 000× to examine cells, and 50 000× to photograph images. Burst size and abundance of visibly infected cells were determined by visual examination (Weinbauer & Suttle 1996). All burst sizes were considered minimal estimates as more particles may have been produced before lysis. Except for a few samples with very low cell abundance, a minimum of 1000 cells was examined for each sample. Because some of the samples from the Sargasso Sea had too few cells to allow complete examination, a subset of the results from several stations were combined and assumed to be constant for all of the Sargasso Sea.

Calculation of % MVL and % IC. The host mortality due to viral lysis (% MVL) was calculated by dividing the rate of viral production by the corresponding minimum burst size to determine the abundance of hosts lysed, and then dividing the quotient by the bacterial standing stock. Percentage of infected cells (% IC) was simply calculated from the percentage of visibly infected cells (VIC) as previously described (Binder 1999) using the following equation:

$$\% \text{ IC} = (7.1) \times (\text{VIC}) - (22.5 \times \text{VIC}^2)$$

Bacterial abundance and production. Bacterial abundance was determined using paraformaldehyde-fixed samples that were filtered onto 0.2 µm pore-size black polycarbonate filters (Porter & Feig 1980) and then stained with a solution containing 1µg ml^{-1} 4′,6-diamidino-2-phenylindole (DAPI) in a phosphate buffer containing 0.5 M NaCl. The filter was mounted on a glass slide with a cover slip and total bacteria (including Archaea and picoplanktonic Cyanobacteria) were enumerated by epifluorescence microscopy using semi-automated image analysis. Bacterial production was estimated from leucine incorporation rates measured by standard methods (Kirchman 2001). Triplicate samples with ^{3}H-leucine (20 nmol l^{-1}) were incubated for 2 h at the *in situ* temperature. The incorporated ^{3}H-leucine was precipitated by trichloroacetic acid (TCA), collected by centrifugation and then rinsed with TCA and ethanol. The samples were then dried and radioassayed to determine ^{3}H-leucine uptake. Killed controls were poisoned with TCA. A conversion factor of 1.5 kg C mol^{-1} of incorporated leucine was used to calculate biomass production.

Bacterial biomass, cell size, and cell volume. Bacterial biomass was estimated from cell abundance data determined by epifluorescence microscopy and semi-automated image analysis of samples stained with 0.5 ng µl^{-1} of DAPI. Cell sizes were estimated from the DAPI image as described previously (Cottrell & Kirchman 2003). Bacterial cell volumes were measured from solids of revolution constructed by digital integration (Sieracki et al. 1989).

Nutrient concentration and regeneration. Concentrations of nitrate + nitrite, ammonium, phosphate and dissolved silicate were determined colorimetrically (Grasshoff et al. 1999) by a standard autoanalyzer (Futura continuous flow analyzer, Alliance Instruments) as soon as the samples were collected at each process station.

To provide an idea of virus-driven nutrient regeneration through both transects, estimates were calculated based on previously determined quotas of C (23.3 fg cell^{-1}) (Simon & Azam 1989), N (5.6 fg cell^{-1}) (Lee & Fuhrman 1987), and Fe (1.1 ag cell^{-1}) (Tortell et al. 1996) released as a result of daily viral lysis within a community.

Statistical correlations. For selected parameters in the Sargasso Sea and North Atlantic, linear regression

of untransformed data was done using software associated with SigmaPlot (ver. 9.0). Since assumptions of normality were not met in distributions of all variables, the nonparametric Spearman Rank Correlation coefficient was calculated as a measure of correlation between all possible pairs of variables. Statistical analysis was done using the NCSS statistical analysis software package. Correlations warranting $p < 0.05$ were considered significant. Multivariate examinations of data were carried out using Canoco (ver. 4.5, Plant Research International). Canonical correspondence analysis (CCA) was performed to determine overall multivariate patterns in the data. Viral production and abundance, bacterial production and abundance, burst size, and cell volume were used as the response (biological) variables, and latitude, total chl *a*, micro-, nano-, pico-chl *a*, salinity, and temperature as the predictor (environmental) variables. Monte Carlo permutation tests confirmed the significance of both canonical correspondence axes.

RESULTS

Size-fractionated chl *a* concentrations along the entire transect reflected an expected trend. Chl *a* was dominated by the picophytoplankton size fraction in the Sargasso Sea, while that in the North Atlantic had variable size distribution and higher concentrations (Fig. 2). Likewise, the abundance of virus-like particles followed a similar trend, with higher viral abundances in North Atlantic waters (Figs. 3A & 4A). Viral abundance in the Sargasso Sea showed a clear increase as the sampling headed northeast. However, the much higher viral abundances in the North Atlantic were highly variable and without a clear trend. Virus-like particle production rates in the Sargasso Sea and North Atlantic (Figs. 3B & 4B) did not follow the same trends as chl *a* concentrations or viral abundance. Production rates in the Sargasso Sea varied from ~0.2×10^8 to 3×10^8 particles h^{-1}, showing a slight increase at stations in the middle of the transect but then decreasing down to the rate which predominated in the North Atlantic. With only one exception, the rates in the North Atlantic remained consistent and at a median level when compared to those of the Sargasso Sea.

The average minimal burst size for the Sargasso Sea (n = 3) was estimated at 11.67 virus-like particles per cell. For the North Atlantic samples, average minimal burst sizes were slightly higher (Fig. 5A) and were not

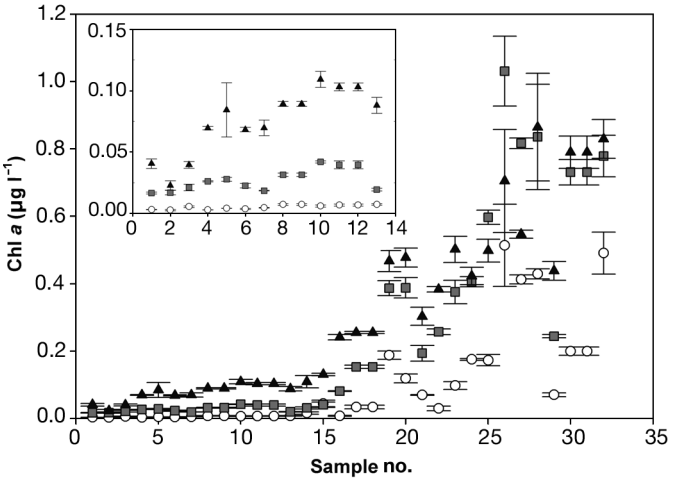

Fig. 2. Size-fractionated chl *a* concentrations in surface water samples (taken along the cruise track) from which viral production assays were performed. Inset is a detailed view of the Sargasso Sea samples. (○) >20.0 µm, (■) 2.0 to 20.0 µm, and (▲) 0.22 to 2.0 µm nominal pore size. Error bars are ranges of duplicate samples

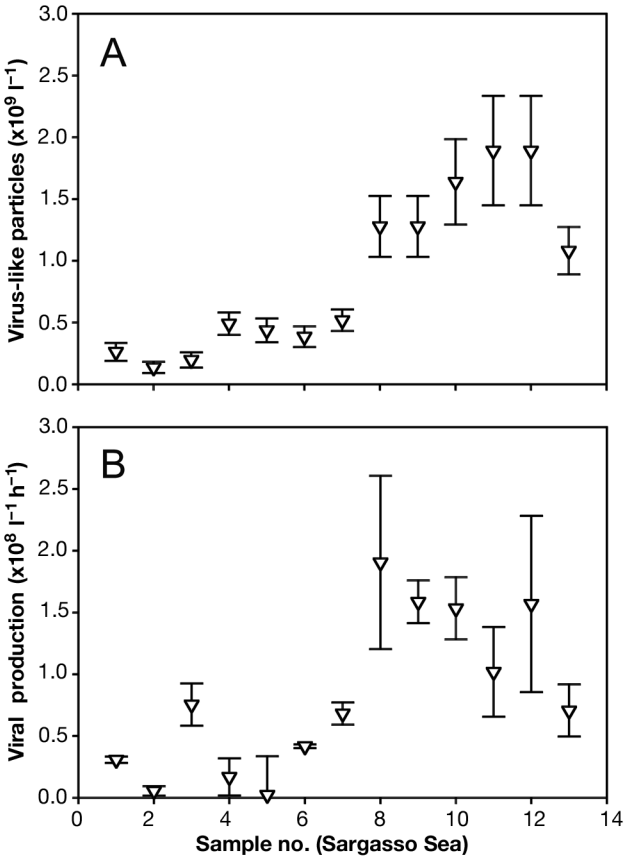

Fig. 3. (A) Virus-like particle abundances in surface water samples taken along the Sargasso Sea transect, from which viral production assays were started. Error bars are variations in virus-like particle counts per field of view after 31 fields were viewed per sample. (B) Viral production rates of surface waters in the Sargasso Sea. Re-appearance of virus-like particles was enumerated over time after free particles were removed. Error bars are SDs of triplicate samples as described in 'Materials and methods'

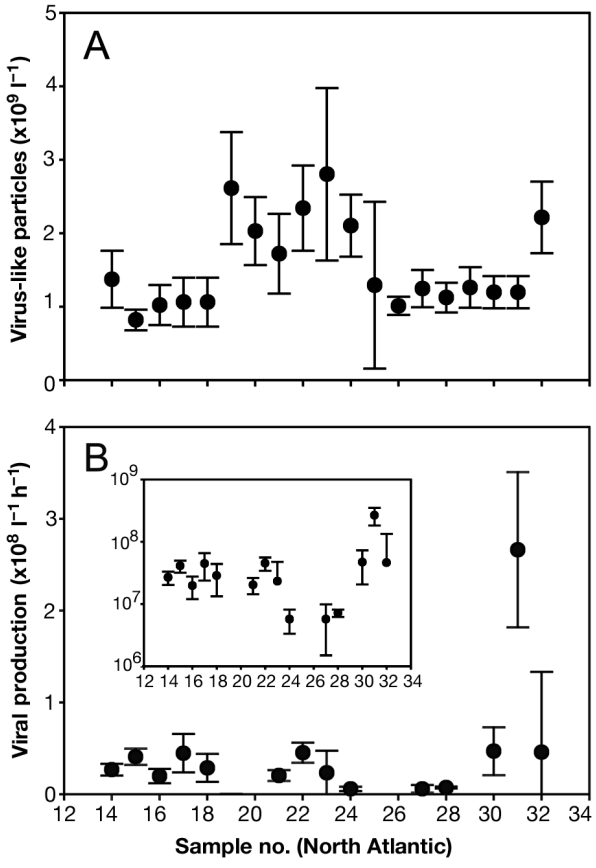

Fig. 4. (A) Virus-like particle abundances in surface water samples taken along the North Atlantic transect, from which viral production assays were started. Error bars are variations in virus-like particle counts per field of view after 31 fields were viewed per sample. (B) Viral production rates of surface waters in the North Atlantic. Re-appearance of virus-like particles was enumerated over time after free particles were removed. Error bars are SDs of triplicate samples as described in 'Materials and methods'. Inset is data plotted on a logarithmic scale

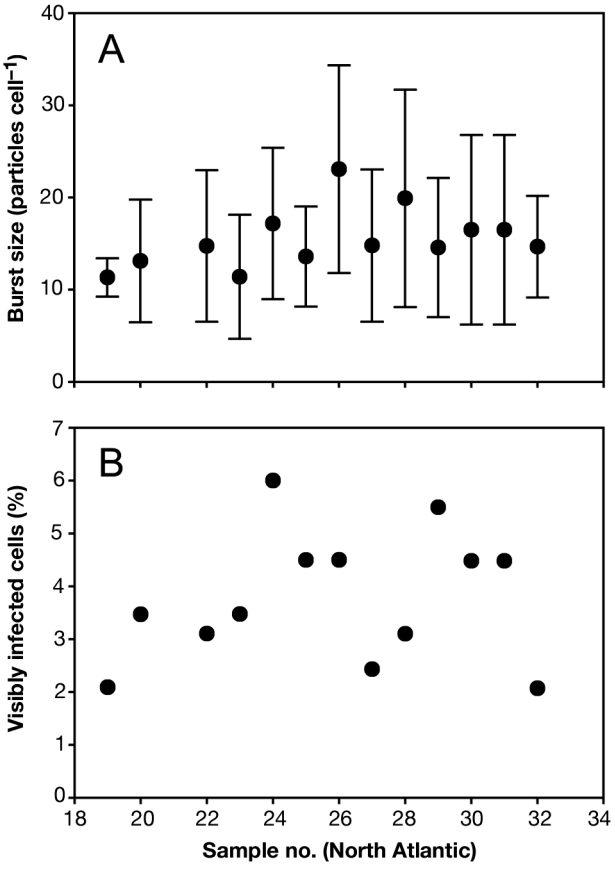

Fig. 5. (A) Minimum burst sizes of infected cells in surface water samples from the North Atlantic. Error bars are variances of virus-like particles per cell within a sample. Sample 21 was lost during processing. (B) Percentage of visibly infected cells taken from surface water samples (North Atlantic) from which viral production assays were performed. Samples were viewed under transmission electron microscopy and analyzed for a minimum of 1000 cells. No variance estimates were generated, as only one sample was analyzed per station. Data from sample 21 not included

significantly different between stations ($p > 0.05$). The percentage of visibly infected cells, however, showed no clear pattern for the North Atlantic samples (Fig. 5B).

To examine how viral production data related to environmental and other biological parameters, we performed several statistical analyses. Linear comparisons of viral production rate and chl *a* concentration (Fig. 6A), viral production rate and viral abundance (Fig. 6B), and viral abundance and chl *a* concentration (Fig. 7) demonstrated no overall correlations between these parameters across both regimes, but allowed for a clearer look at each separate regime. Results from the Sargasso Sea suggested a strong positive relationship between viral abundance and chl *a* concentrations (Fig. 7) ($r^2 = 0.832$, $p < 0.001$), and to a lesser extent between production rate and abundance (Fig. 6B) ($r^2 = 0.630$, $p = 0.0012$). Although no significant linear relationships in the same parameters were evident in the North Atlantic results, 2 trends were made evident in Fig. 6; a constant narrow range of viral production rate during large changes in chl *a* and in viral abundance. Additionally, we examined the ratio of viral to bacterial abundances for the Sargasso Sea (Fig. 8A) and the North Atlantic (Fig. 8B). Again, a statistically significant linear relationship was evident in the Sargasso Sea ($r^2 = 0.830$, $p < 0.001$), but not in the North Atlantic.

Because only a subset of the data analyzed is being discussed, an abbreviated set of the Spearman Rank Correlation analyses is given in Table 1. To simplify this massive dataset, relationships where no statistical significance was observed are not shown. Although a strong correlation between silicate and virus-like particle abundance was observed, no relationship was

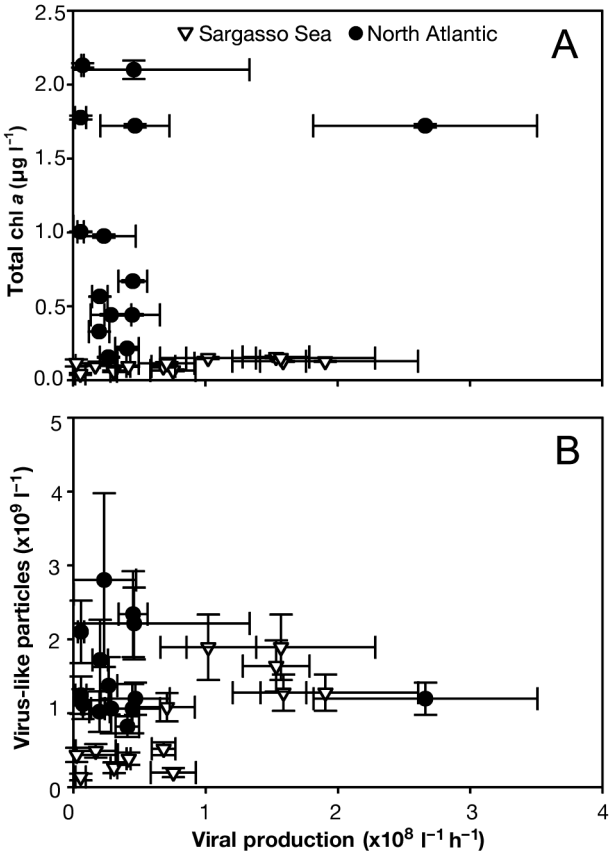

Fig. 6. (A) Virus-like particle production rates vs. total chl *a* concentrations and (B) virus-like particle production rates vs. virus-like particle abundances for the Sargasso Sea and the North Atlantic. For both (A) and (B), all North Atlantic samples (except for sample no. 31) group together and separately from Sargasso Sea samples, which also group together. The linear relationship of the Sargasso Sea samples has an r^2 of 0.630 ($p = 0.0012$)

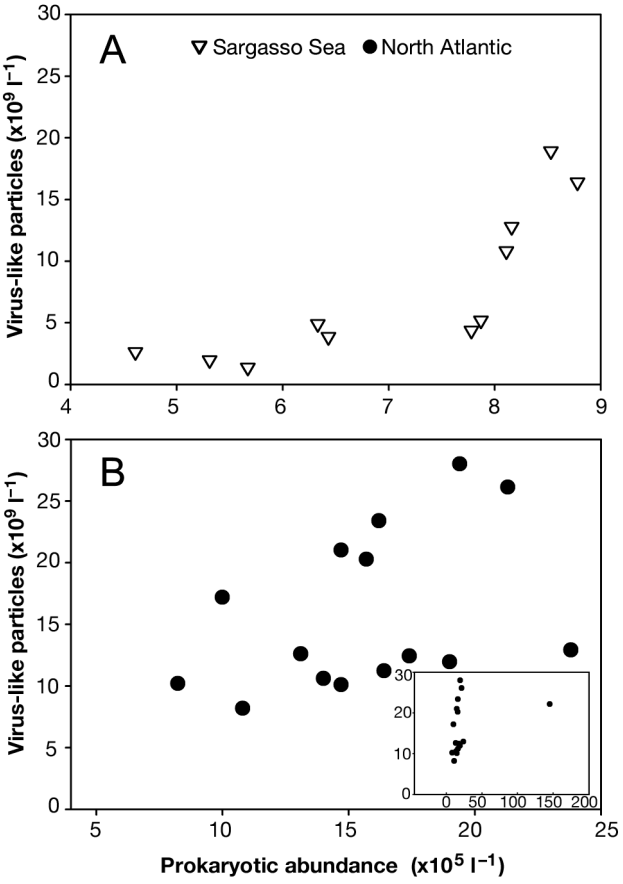

Fig. 8. Viral vs. bacterial abundance in stations along the (A) Sargasso Sea, and (B) North Atlantic transects. Results show that bacterial abundance is a better predictor of viral abundance in the Sargasso Sea ($r^2 = 0.690$, $p < 0.001$) than in the North Atlantic ($r^2 = 0.137$, $p > 0.05$). North Atlantic data were analyzed without one outlier (sample 32, included in inset)

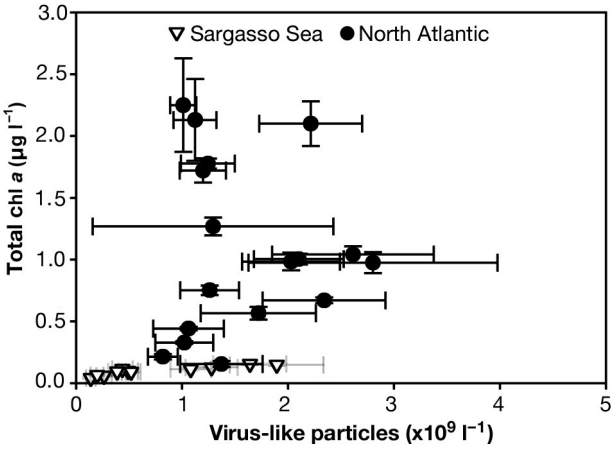

Fig. 7. Virus-like particle abundances vs. total chl *a* concentrations for the Sargasso Sea and the North Atlantic. Linear regression of Sargasso Sea samples has an r^2 of 0.832 ($p < 0.001$)

noted between viral abundance and the other nutrients measured. The large number of significant relationships ($p \leq 0.05$) between viral parameters and other biological estimates are discussed below.

Viruses were estimated to be responsible for the daily regeneration of ~9 to 761 nM of organic C, 1.9 to 157 nM of organic N, and 0.1 to 8 pM of organic Fe within the Sargasso Sea, with similar levels of activity in the North Atlantic (Table A1; see Appendix 1, available in AME Supplementary Material at www.int-res.com/articles/suppl/a052p233_app.pdf). Results shown are for each station where viral production rates were also determined.

CCA performed to determine overall multivariate patterns in the data, and Monte Carlo permutation tests that confirmed the significance of both canonical correspondence axes revealed the data to be in 2 clusters; one for the Sargasso Sea, and one for the

Table 1. Spearman rank correlation analysis contrasting viral production rates (VP) and viral abundance (VA) with biotic and abiotic parameters. Significant relationships ($p < 0.05$) are given in bold. ND = not determined, r_s = correlation coefficient, VIC = visibly infected cells

Parameter	Entire transect				Sargasso Sea only				North Atlantic only			
	VP		VA		VP		VA		VP		VA	
	r_s	p	r_s	p	r_s	p	r_s	p	r_s	p	r_s	p
Viral abundance	0.028	0.882	x	x	0.725	**0.005**	x	x	−0.052	0.842	x	x
Chl *a*												
Total (>0.2 µm)	−0.438	**0.014**	0.533	**0.002**	0.653	**0.016**	0.923	**<0.001**	−0.288	0.262	0.156	0.536
0.2 – 2.0 µm	−0.391	**0.030**	0.553	**<0.001**	0.686	**<0.001**	0.967	**<0.001**	−0.132	0.615	0.225	0.371
> 20 µm	−0.383	**0.033**	0.499	**0.004**	0.852	**<0.001**	0.730	**0.005**	−0.276	0.284	0.088	0.728
2.0–20.0 µm	−0.417	**0.030**	0.524	**0.002**	0.625	**0.022**	0.818	**<0.001**	−0.273	0.289	0.142	0.575
Bacterial abundance	−0.389	**0.037**	0.664	**<0.001**	0.702	**0.007**	0.945	**<0.001**	−0.191	0.478	0.516	**0.034**
Bacterial production	−0.392	**0.036**	0.409	**0.025**	0.572	0.052	0.789	**0.002**	0.087	0.740	−0.111	0.662
Cell volume	−0.382	**0.037**	0.257	0.163	−0.267	0.377	0.006	0.986	−0.276	0.284	0.382	0.118
Burst size	−0.263	0.152	−0.013	0.946	0.000	1.000	0.000	1.000	0.233	0.367	−0.646	**0.004**
Salinity	0.448	**0.028**	−0.455	**0.022**	−0.117	0.748	−0.511	0.131	0.155	0.597	0.163	0.562
North Atlantic only												
% VIC	–	–	–	–	ND	ND	ND	ND	−0.283	0.373	−0.278	0.357
Ammonium	–	–	–	–	ND	ND	ND	ND	0.334	0.190	0.305	0.218
Nitrate/Nitrite	–	–	–	–	ND	ND	ND	ND	−0.298	0.245	0.229	0.362
Phosphate	–	–	–	–	ND	ND	ND	ND	−0.158	0.545	0.331	0.180
Silicate	–	–	–	–	ND	ND	ND	ND	0.072	0.783	0.808	**<0.001**

North Atlantic, indicating that these are biologically different systems (Fig. A1 in Appendix 1). Redundancy analysis was also done using the same biological and environmental variables as for the CCA. This linear model also revealed a separation of Sargasso Sea and North Atlantic data (Fig. A2 in Appendix 1), supporting the CCA results.

DISCUSSION

During the NASB 2005 project, we had the opportunity to collect samples from 54 characterized stations in the North Atlantic. As part of this study, we were also able to collect a subset of data during the transit run from Florida to the Azores. While the latter data was less complete than the data set for the North Atlantic, the results of both surveys are included in this paper in an attempt to shed some light on differences in the production, abundance, and estimated effects of viruses in these well-defined and trophically different systems.

Although interest in viral ecology has grown significantly in recent years, the factors which constrain the rates of viral production in aquatic systems have remained elusive (Suttle 2005, Brussaard et al. 2008, Wilhelm & Matteson 2008). Our data demonstrate that viral production rates are better predicted by common oceanographic parameters (e.g. chl *a*, viral abundance) in the Sargasso Sea than in the North Atlantic. The constraints on viral production within the less dynamic Sargasso appear to be a function of the relatively constant and comparably low abundance and diversity of the potential host population that contain both heterotrophic and phototrophic cells (Ducklow et al. 1993, Harrison et al. 1993, Steinberg et al. 2001, this study). In the more dynamic North Atlantic, with its episodic and transitory phytoplankton blooms, viral production rates appear to hold a more complex relationship with the coexisting biotic and abiotic factors. This relationship suggests a possible threshold effect of lesser known constraints on viral production and abundance that act/become more significant after thresholds have been reached by factors of greater impact. These situations render pair-wise analyses less effective and emphasize the need for methods and statistical analyses which can tease apart the true multi-factor relationships, including those involving specific virus-host populations.

Chl *a* concentrations measured over the length of the cruise reflect the disparate biomass of primary producers in these 2 oceanic systems. The oligotrophic Sargasso Sea was predictably dominated by picophytoplankton (Li et al. 1992) and the nutrient-rich North Atlantic was dominated by a series of events collectively termed the NASB (Martin et al. 1993). Abundance of viruses in both

regimes reflected the expected trends based on previous examinations of oligotrophic and mesotrophic marine waters (Wommack & Colwell 2000). Abundance increased in more productive waters, but reached a plateau at the most productive stations, suggesting that a stable dynamic between the factors influencing virus-like particle appearance and decay had been reached (Wilhelm et al. 1998a, Weinbauer et al. 1999). Although total virus-like particle abundances remained within a narrow range in the North Atlantic samples, this does not necessarily indicate an unchanging viral community as turnover rates were high. It is likely that a change in host community structure would be mirrored by a change in the viral community structure, although this was outside the scope of the current study.

In this study, viral production assays were always carried out under *in situ* light conditions to reduce artificially imposed limits and to ensure accurate inclusion of viruses infecting phototrophic organisms. As such, most of the rates observed were within the ranges seen in other studies (Weinbauer et al. 2002, Wilhelm et al. 2002, Poorvin et al. 2004, Winter et al. 2004), although our highest estimate (from Stn 31) was an order of magnitude greater than rates observed in other systems, suggesting that this may be an outlier. Viral abundance and production rates in the Sargasso Sea transect increased as sampling progressed from the gyre into more productive waters. However, as we moved into North Atlantic waters, both abundance and production rates leveled off. Although it was not surprising to see an increase in viral production in waters of increased system productivity, that viral abundance and production remained constant during sampling across different algal bloom stages and across changes in community structure was not expected. These results suggest that the effects of system productivity on viral proliferation may have reached an upper limit (a threshold effect), leaving traditionally less influential factors responsible for minor fluctuations. Although this resulted in an apparent lack of relationship between system productivity and viral parameters, monitoring of changes in system productivity and viral parameters over such a large scale (2 distinct oceanic regimes) has provided us with a far more complete picture than would have been obtained from examining the North Atlantic system alone. It is not logical to assume that the relationships between system productivity and viral parameters would become insignificant or even suddenly cease to exist without some other factor or set of factors exerting influence.

Burst size estimates for lytic events in both the Sargasso Sea and North Atlantic were low in this study, ranging from ~11 to 25. Historically, estimates of burst size used in calculations of virus-inferred mortality have been high (up to ~500), and were based on estimates taken from observations of primarily coastal populations (Wommack & Colwell 2000, Weinbauer 2004). While burst sizes were relatively invariant in the North Atlantic, the percentage of visibly infected cells fluctuated between 2 and 6% with no apparent pattern. These results indicate that there are factors that influence the rates of infection and lysis. Infection rate is most affected by contact rates and host density, while burst size depends on initial cell size and/or host metabolism, as well as viral particle size (Weinbauer 2004).

Cells in the Sargasso Sea samples were too sparse to allow estimation of the percentage of visibly infected cells at each station, but a collectively estimated burst size was clearly lower than those determined for the North Atlantic. The lower production of the Sargasso Sea could explain the lower burst size. Host cells may not have sufficient energy or nutrients to package as many viral particles as their counterparts in more productive waters. That bacterial burst sizes in the North Atlantic were higher, yet fairly constant, could be an indicator that host metabolism in this system had reached influential maxima. It has been accepted that system productivity via host metabolism is a significant factor limiting burst size (Weinbauer 2004). The fluctuating percentages of visibly infected cells in the North Atlantic could have been due to changes in specific host cell density and/or diversity.

Regulators of viral production

To examine how viral parameters relate to one another as well as to environmental variables, pair-wise correlations were first examined for all data followed by a more in-depth examination using Spearman Rank Correlation analyses. This analysis does not make assumptions on how the data are distributed (e.g. normal as in parametric analyses) and is therefore more suitable for analyzing results from natural samples. The multivariate approach (CCA) used to assess the grouping of North Atlantic and Sargasso Sea data (those common in both transects) was chosen because it is unimodal (i.e. does not assume linear relationships, allowing for data to find an optimum along a gradient) and constrained (i.e. allows axes to be made from the known environmental parameters to better show relationships). In short, CCA provided the statistical backing to differentiate the North Atlantic oceanic regime from that of the Sargasso Sea, allowing us to separate these transects for parametric and non-parametric analyses discussed below. Redundancy analysis, which uses a linear species distribution model, also showed that the data fell in 2 distinct clusters. This analysis was performed to see any differences between unimodal and linear models of data

representation. Both analyses, however, did not yield any multivariate relationships within or between the biological and environmental parameters examined.

Within the parametric analyses, viral production rate vs. total chl *a*, viral abundance vs. chl *a*, and viral production rate vs. viral abundance were of sufficient interest to present and discuss. From these 3 comparisons, we see different trends in the data depending on sample location. Correlations between viral production rates and chl *a* have been suggested to be due to the linkage between primary production rates and overall ecosystem energetics (Maranger & Bird 1995). In our study, viral production was positively correlated to chl *a* for the Sargasso Sea data set. In the North Atlantic, rates of viral production were relatively constant, and as such appeared independent of changes in phytoplankton biomass (chl *a*). Many new hypotheses arise from these observations, with the relative simplicity and stability of the system in question potentially being of great importance. The Sargasso Sea, with sparse host population abundance, minimal water movement (i.e. no interior currents), and persistent sunlight which can induce UV damage in viral particles (Wilhelm et al. 1998b), is an environment where viral production rates are most likely to be closely dependent on system energetics. In contrast, the North Atlantic is an environment where biological processes are more dynamic; periods of low productivity are contrasted by the significant bloom events of the NASB, and multiple currents provide mixing and turbulence as well as importation of nutrients (Ducklow & Harris 1993, Gregg 2002, Faure & Speer 2005, Limeburner et al. 2005). Factors controlling viral production within this region may thus be more complicated and intertwined. Transient changes in host populations along with changes in water column chemistry and mixing undoubtedly lead to rapid seasonal cycling of viral populations ('boom and bust'), somewhat contrasting with Thingstad & Lignell's (1997) 'kill the winner' hypothesis. Other factors such as the transient nature of water column clarity (due to biological fluctuations and mixing) in this region may influence processes such as UV-mediated decay. The decay rate of viral particles was not examined in this study.

In contrast to previous efforts, our study included rates of production of virus-like particles infectious to both algae and bacteria (as estimates were made at *in situ* light levels and not in the dark). Weinbauer (2004) has previously suggested that correlations between viral and bacterial abundance exist primarily because most viruses are believed to infect bacteria. In our study, analysis of virus to bacterium abundance ratios suggests that a relationship exists for the Sargasso Sea (Fig. 8A) (r^2 = 0.690) but not for the North Atlantic (Fig. 8B) (r^2 = 0.137). However, again the grouping of data points across both regimes suggests that a threshold effect comes into play when bacterial abundance reaches 8×10^5, perhaps explaining why no apparent relationship exists between these 2 parameters when looking solely at the North Atlantic data. It thus appears that viral production in the Sargasso is a function of bacterial activity and abundance. However, the strong correlation between viral abundance and chl *a* (Fig. 7) indicates that viral production is also a function of primary production and biomass, and this is supported by the significant correlation between viral abundance and viral production (Table 1) for the Sargasso Sea data. The same correlations may exist for the North Atlantic, but the higher primary and heterotrophic production rates may have masked the correlation of viral parameters to bacterial parameters and vice versa. This does not reject the possibility of a threshold effect as discussed earlier, which may be another complicating factor to this mixture of viral and system parameters. Overall differences between the 2 data sets clearly show that relationship patterns are regime dependent, and that analyses must examine data separately as well as collectively.

For the entire data set for both regimes, all of the biological parameters except burst size correlate significantly with viral production rates. Correlations with viral abundance are similarly significant except for cell volume. Further examination of the data, however, suggests that the combined observations are driven by the Sargasso Sea data, with only bacterial and viral abundance correlating significantly in the North Atlantic samples (although not under normal distribution as discussed previously). In all, these observations support the contention that viral abundance and production in the constant Sargasso Sea environment are more predictable than in the dynamic North Atlantic system.

Also notable are several observations of weak, yet significant correlations that cannot be adequately explained due to limited sample size and range (Table 1). In the entire data set, but not for either of the individual transects, bacterial cell volume was negatively related to viral production, but not to abundance. Burst size displayed a negative relationship to viral abundance in the North Atlantic samples. It remains surprising that burst size and the percentage of visibly infected cells did not correlate with virus-like particle production rate or with abundance. One possibility is that burst size only influences viral abundance and production within certain limits (i.e. to the degree that host diversity and trophic status control the abundance of viruses produced). As suggested for marine phytoplankton, the available nucleotide resources may be of more direct influence on burst size (Brown et al. 2006), but genome sizes were not analyzed here. Cell size

could be an indicator of the cell's ability to produce virus-like particles, with larger cells potentially having more energy stores to utilize and/or more machinery. This is also supported by the significant relationship between bacterial production and virus-like particle production rates and abundances. More studies focused on this area would be of value in learning the exact nature of the relationship between cell size and viral production. Indeed, given the constancy of our observations across these 2 regimes, our results indicate that viral production rate and abundance may be largely independent of the number of particles released during cell lysis.

Viral interactions with system geochemistry

In the combined data set, analyses demonstrate that viral abundance and production are tightly coupled to the biological parameters examined, yet are only significantly correlated to one geochemical parameter (silicic acid). However, estimates from this study suggest that viruses in both regimes regenerate significant concentrations of dissolved organic C as well as trace elements (as shown for N and Fe). These results support the growing evidence that viruses are major drivers of the nutrient regeneration that supports >70% of marine productivity (Raven & Falkowski 1999), and that viral productivity is tied directly to biological rather than biogeochemical processes (Poorvin et al. 2004).

Dissolved silicate concentrations in the North Atlantic had a strongly significant positive correlation with viral abundance but not with production (r_s = 0.808, $p < 0.001$) in the Spearman analysis. We hypothesize that nutrient usage by primary producers would likely lead to increased cellular metabolism, and subsequently increase viral production rates and abundance. However, the lack of relationship between the viral parameters and nearly all of the nutrients suggests a disconnect between viral production rates and abundance from the trophic status of the North Atlantic. In part, this may be explained by nutrient concentrations that are subject to the episodic bloom events described above. In the case of the relationship between viral abundance and silicate, these results suggest that correlations between viral abundance and diatom proliferation may be strong and negative (floristic data is not currently available). Viral infection of diatoms in marine waters has rarely been documented, and viruses have only recently been characterized for a few diatoms (Nagasaki et al. 2004, 2005). However, for other algae in this ecosystem (e.g. *Emiliania huxleyi*), viral infection has been very well studied and is thought to be common (Schroeder et al. 2003, Evans et al. 2007). As such, the correlation between high dissolved silicate and high viral abundance and production rates is probably a reflection of the role of viruses in the regulation of populations of algae other than diatoms when diatom densities are too low to draw down dissolved silicate.

While system geochemistry appears to influence viral abundance and production, it is well known that viral activity also influences system geochemistry. In this study, viruses were estimated to be responsible for the daily regeneration of ~9 to 761 nM of organic C, 1.9 to 157 nM of organic N and 0.1 to 8 pM of organic Fe within the Sargasso Sea, with similar levels of activity in the North Atlantic (Table A1 in Appendix 1). While the amount of organic C (dissolved and particulate) recycled by viral activity is small compared to the 68 to 78 µM DOC pool in the Sargasso Sea (Carlson & Ducklow 1996), this pool should include a labile fraction which is highly bioavailable to the microbial community (Middelboe & Jörgensen 2006).

Perhaps more significant are the concentrations of N and Fe which are recycled back into the water column during the lysis of host cells. Previous studies have demonstrated that the vast majority of Fe released during virus-mediated cell lysis is organically bound (Poorvin et al. 2004). It can be anticipated that most of the N released is organic as well. Viral activity may thus drive biogeochemical pathways that favor organic rather than inorganic nutrient cycles, ultimately influencing community structure and diversity. Fe released by virus-mediated cell lysis (and other mechanisms such as grazing) has been shown to be highly bioavailable to various marine plankton (Gobler et al. 1997, Poorvin et al. 2004, Mioni et al. 2005). Therefore, it may be rapidly recycled even though it represents only 1 to 3% of the total dissolved Fe concentrations that have been previously measured in this system (Wu & Boyle 2002).

In summary, this study has provided insights on how virus-host interactions are affected by environmental parameters, and how the constraints on viral abundance and production may be a function of the stability of the regime being considered (constant vs. dynamic). The ability of viruses to respond to their environment highlights the adaptability of these obligate pathogens. Indeed, if we were to readdress previous efforts to understand how different plankton communities are structured (Hutchinson 1961), it becomes apparent that regardless of the trophic status or temporal stability, viruses must play a significant role in the outcome. The adoption of novel molecular tools which can more specifically address processes and functions associated with individual viral groups will, in the future, address many of the other questions raised over the course of this investigation.

Acknowledgements. We thank the Captain and crew of the RV 'Seward Johnson' as well as M. Carberry, G. DiTullio, C. Hare, and other scientists on the NASB2005 cruise. The paper was improved by comments from 2 anonymous reviewers and the editor. This research was funded by grants from the National Science Foundation to D.A.H. (OCE 0423418), D.L.K. (OCE 0452377) and S.W.W. (OCE 0452409).

LITERATURE CITED

Balch WM, Kilpatrick KA, Trees CC (1996) The 1991 coccolithophore bloom in the central North Atlantic. 1. Optical properties and factors affecting their distribution. Limnol Oceanogr 41:1669–1683

Binder B (1999) Reconsidering the relationship between virally induced bacterial mortality and frequency of infected cells. Aquat Microb Ecol 18:207–215

Brown CM, Lawrence JE, Campbell DA (2006) Are phytoplankton population density maxima predictable through analysis of host and viral genomic DNA content? J Mar Biol Assoc UK 86:491–498

Brussaard CPD, Wilhelm SW, Thingstad F, Weinbauer MG and others (2008) Global-scale processes with a nanoscale drive: the role of marine viruses. ISME J 2:575–578

Carlson CA, Ducklow HW (1996) Growth of bacterioplankton and consumption of dissolved organic carbon in the Sargasso Sea. Aquat Microb Ecol 10:69–85

Cottrell MT, Kirchman DL (2003) Contribution of major bacterial groups to bacterial biomass production (thymidine and leucine incorporation) in the Delaware estuary. Limnol Oceanogr 48:168–178

DeBruyn JM, Leigh-Bell JA, McKay RML, Bourbonniere RA, Wilhelm SW (2004) Microbial distributions and the impact of phosphorus on bacterial activity in Lake Erie. J Gt Lakes Res 30:166–183

Ducklow HW, Harris RP (1993) Introduction to the JGOFS North Atlantic bloom experiment. Deep-Sea Res II 40:1–8

Ducklow HW, Kirchman DL, Quinby HL, Carlson CA, Dam HG (1993) Stocks and dynamics of bacterioplankton carbon during the spring bloom in the eastern North Atlantic Ocean. Deep-Sea Res II 40:245–263

Duckworth DH (1976) Who discovered bacteriophage? Bacteriol Rev 40:793–802

Evans C, Kadner SV, Darroch LJ, Wilson WH, Liss PS, Malin G (2007) The relative significance of viral lysis and microzooplankton grazing as pathways of dimethylsulfoniopropionate (DMSP) cleavage: an *Emiliania huxleyi* culture study. Limnol Oceanogr 52:1036–1045

Faure V, Speer K (2005) Labrador Sea water circulation in the northern North Atlantic Ocean. Deep-Sea Res II 52: 565–581

Fuhrman JA (1992) Bacterioplankton roles in cycling of organic matter: the microbial food web. In: Falkowski PG, Woodhead A (eds) Primary productivity and biogeochemical cycles in the sea. Plenum, New York, p 361–384

Gobler CJ, Hutchins DA, Fisher NS, Cosper EM, Sãnudo-Wilhelmy SA (1997) Release and bioavailability of C, N, P, Se, and Fe following viral lysis of a marine chrysophyte. Limnol Oceanogr 42:1492–1504

Grasshoff K, Ehrhardt M, Kremling K (1999) Methods of seawater analysis. Wiley-VCH Verlag, New York

Gregg WW (2001) Tracking the SeaWiFS record with a coupled physical/biogeochemical/radiative model of the global oceans. Deep-Sea Res II 49:81–105

Harrison WG, Head EJH, Horne EPW, Irwin B, Li WKW, Longhurst AR, Paranjape MA, Platt T (1993) The western North Atlantic bloom experiment. Deep-Sea Res II 40: 279–305

Hutchinson GE (1961) The paradox of the plankton. Am Nat 95:137–145

Kirchman DL (2001) Measuring bacterial biomass production and growth rates from leucine incorporation in natural aquatic environments. Method Microbiol 20:227–236

Lee S, Fuhrman JA (1987) Relationships between biovolume and biomass of naturally derived marine bacterioplankton. Appl Environ Microbiol 53:1298–1303

Li WKW, Dickie PM, Irwin BD, Wood AM (1992) Biomass of bacteria, cyanobacteria, prochlorophytes and photosynthetic eukaryotes in the Sargasso Sea. Deep-Sea Res 39:501–519

Limeburner R, Whitehead JA, Cenedese C (2005) Variability of Antarctic bottom water flow into the North Atlantic. Deep-Sea Res II 52:495–512

Maranger R, Bird DF (1995) Viral abundances in aquatic systems: a comparison between marine and fresh waters. Mar Ecol Prog Ser 121:217–226

Martin JH, Fitzwater SE, Gordon RM, Hunter CN, Tanner SJ (1993) Iron, primary production and carbon-nitrogen flux studies during the JGOFS North Atlantic bloom experiment. Deep-Sea Res II 40:115–134

Middelboe M, Jörgensen NOG (2006) Viral lysis of bacteria: an important source of dissolved amino acids and cell wall compounds. J Mar Biol Assoc UK 86:605–612

Mioni CE, Poorvin L, Wilhelm SW (2005) Virus and siderophore-mediated transfer of available Fe between heterotrophic bacteria: characterization using an Fe-specific bioreporter. Aquat Microb Ecol 41:233–245

Nagasaki K, Tomaru Y, Katanozaka N, Shirai Y, Nishida K, Itakura S, Yamaguchi M (2004) Isolation and characterization of a novel single-stranded RNA virus infecting the bloom-forming diatom *Rhizosolenia setigera*. Appl Environ Microbiol 70:704–711

Nagasaki K, Tomaru Y, Takao Y, Nishida K, Shirai Y, Suzuki H, Nagumo T (2005) Previously unknown virus infects marine diatom. Appl Environ Microbiol 71:3528–3535

Noble RT, Fuhrman JA (1998) Use of SYBR Green I for rapid epifluorescence counts of marine viruses and bacteria. Aquat Microb Ecol 14:113–118

Poorvin L, Rinta-Kanto JM, Hutchins DA, Wilhelm SW (2004) Viral release of Fe and its bioavailability to marine plankton. Limnol Oceanogr 49:1734–1741

Porter KG, Feig YS (1980) The use of DAPI for identifying and counting aquatic microflora. Limnol Oceanogr 25:943–948

Raven JA, Falkowski PG (1999) Oceanic sinks for atmospheric CO_2. Plant Cell Environ 22:741–755

Schroeder DC, Oke J, Hall M, Malin G, Wilson WH (2003) Virus succession observed during an *Emiliania huxleyi* bloom. Appl Environ Microbiol 69:2484–2490

Sieracki ME, Reichenbach SE, Webb KL (1989) Evaluation of automated threshold selection methods for accurately sizing microscopic fluorescent cells by image analysis. Appl Environ Microbiol 55:2762–2772

Sieracki ME, Verity PG, Stoecker DK (1993) Plankton community response to sequential silicate and nitrate depletion during the 1989 North Atlantic spring bloom. Deep-Sea Res II 40:213–225

Simon M, Azam F (1989) Protein content and protein synthesis rates of planktonic marine bacteria. Mar Ecol Prog Ser 51:201–213

Steinberg DK, Carlson CA, Bates NR, Johnson RJ, Michaels AF, Knap AH (2001) Overview of the US JGOFS Bermuda Atlantic Time-series Study (BATS): a decade-scale look at ocean biology and biogeochemistry. Deep-Sea Res II 48:1405–1447

Suttle CA (2005) Viruses in the sea. Nature 437:356–361

Thingstad TF, Lignell R (1997) Theoretical models for the control of bacterial growth rate, abundance, diversity and carbon demand. Aquat Microb Ecol 13:19–27

Tortell PD, Maldonado MT, Price NM (1996) The role of heterotrophic bacteria in iron-limited ocean ecosystems. Nature 383:330–332

Weinbauer MG (2004) Ecology of prokaryotic viruses. FEMS Microbiol Rev 28:127–181

Weinbauer MG, Suttle CA (1996) Potential significance of lysogeny to bacteriophage production and bacterial mortality in coastal waters of the Gulf of Mexico. Appl Environ Microbiol 62:4374–4380

Weinbauer MG, Wilhelm SW, Suttle CA, Pledger RJ, Mitchell DL (1999) Sunlight-induced DNA damage and resistance in natural viral communities. Aquat Microb Ecol 17: 111–120

Weinbauer MG, Winter C, Höfle MG (2002) Reconsidering transmission electron microscopy based estimates of viral infection of bacterioplankton using conversion factors derived from natural communities. Aquat Microb Ecol 27:103–110

Welschmeyer NA (1994) Fluorometric analysis of chlorophyll *a* in the presence of chlorophyll *b* and phaeopigments. Limnol Oceanogr 39:1985–1992

Wen K, Ortmann AC, Suttle CA (2004) Accurate estimation of viral abundance by epifluorescence microscopy. Appl Environ Microbiol 70:3862–3867

Wilhelm SW, Matteson AR (2008) Freshwater and marine virioplankton: a brief overview of commonalities and differences. Freshw Biol 53:1076–1089

Wilhelm SW, Suttle CA (1999) Viruses and nutrient cycles in the sea. BioScience 49:781–788

Wilhelm SW, Weinbauer MG, Suttle CA, Jeffrey WH (1998a) The role of sunlight in the removal and repair of viruses in the sea. Limnol Oceanogr 43:586–592

Wilhelm SW, Weinbauer MG, Suttle CA, Pledger RJ, Mitchell DL (1998b) Measurements of DNA damage and photoreactivation imply that most viruses in marine surface waters are infective. Aquat Microb Ecol 14: 215–222

Wilhelm SW, Brigden SM, Suttle CA (2002) A dilution technique for the direct measurement of viral production: a comparison in stratified and tidally mixed coastal waters. Microb Ecol 43:168–173

Wilhelm SW, Jeffrey WH, Dean AL, Meador J, Pakulski JD, Mitchell DL (2003) UV radiation induced DNA damage in marine viruses along a latitudinal gradient in the southeastern Pacific Ocean. Aquat Microb Ecol 31:1–8

Winget DM, Williamson KE, Helton RR, Wommack KE (2005) Tangential flow diafiltration: an improved technique for estimation of virioplankton production. Aquat Microb Ecol 41:221–232

Winter C, Herndl GJ, Weinbauer MG (2004) Diel cycles in viral infection of bacterioplankton in the North Sea. Aquat Microb Ecol 35:207–216

Wommack KE, Colwell RR (2000) Virioplankton: viruses in aquatic ecosystems. Microbiol Mol Biol Rev 64:69–114

Wu JF, Boyle E (2002) Iron in the Sargasso Sea: implications for the processes controlling dissolved Fe distribution in the ocean. Global Biogeochem Cycles 16:1086 doi: 10.1029/2001GB001453

Editorial responsibility: Gunnar Bratbak, Bergen, Norway

Submitted: March 7, 2008; Accepted: June 2, 2008
Proofs received from author(s): August 29, 2008